Supplemental Information

Autistic-like phenotypes in *Cadps2*/*CAPS2* knockout mice and aberrant *CADPS2* splicing in autistic patients

Tetsushi Sadakata, Miwa Washida, Yoshimi Iwayama, Satoshi Shoji, Yumi Sato, Takeshi Ohkura, Ritsuko Katoh-Semba, Mizuho Nakajima, Yukiko Sekine, Mika Tanaka, Kazuhiko Nakamura, Yasuhide Iwata, Kenji J. Tsuchiya, Norio Mori, Sevilla D. Detera-Wadleigh, Hironobu Ichikawa, Shigeyoshi Itohara, Takeo Yoshikawa, Teiichi Furuichi

Supplemental Methods

Behavioral tests. All experimental protocols were approved by the RIKEN Institutional Animal Care and Use Committee. Mice were housed on a 12:12 h LD cycle, with the dark cycle occurring from 20:00 to 8:00. All mice used in the experiments below were littermates from mated heterozygotes. The experimenter was blind to the genotype in all behavioral tests.

Vision test: The vision test was performed as previously described (63). Male mice (*n*=8 of each genotype) were held by their tails 30 cm above and about 5 cm out from the surface of a table in the light phase of the light cycle. They were slowly lowered so that they would pass close to the edge of the table, but far enough away so that their whiskers would not touch the table surface. Mice with vision reach for the table as they are lowered past the surface of the table.

Hidden-cookie test: The hidden-cookie test was performed as previously described (63). Male mice (*n*=8 of each genotype) were food-deprived overnight. A piece of butter cookie (Morinaga, Inc., <0.7 g/piece) was buried beneath about 3 cm of clean bedding in a random location. The mouse was placed in the cage, again in a random location, in the light phase of the light cycle. The latency time to locate the cookie was recorded. We defined finding the cookie as when the mouse held it in both paws.

Acoustic startle response: The acoustic startle response was examined as previously described (64) with minor modifications. The apparatus used for recording acoustic startle response was a 6.6 x 4.6 x 4.6 cm acryl mouse container. It was placed in a sound-attenuation box. The startle stimulus was generated by an audio stimulator (cat. no. ANL-925, Med Associates). The stimulus was delivered by a tweeter, which was located 15 cm above the ceiling of the animal container. The luminescent level at the position of the animal container was 40 lux. After a 3-min adaptation period, the startle experiment was begun. The white noise was presented at 70 dB for a duration of 15 s. The horizontal movements were monitored with a CCD camera. The images were processed with NIH IMAGE FZ software (O'Hara & Co.). The percentage change of movements to the sound stimulus was calculated by the ratio of the movement during the sound stimulus (15 s) to that for 15 s prior to the stimulus.

Morris water maze test: The Morris water maze test was conducted as previously described (65) with minor modifications. The mice used in this test were 5-week-old males. The water pool used in these experiments was 1 m in diameter and made of white polyvinyl chloride. The temperature of the water was held constant at 25 ± 1^{o}C. On the first day of training, mice were tested in a visible platform task four times. In this task, the platform was made visible by attaching a black cubic landmark to the platform. In the hidden-platform task, the acrylic transparent platform (diameter 10 cm) was submerged 1 cm below the surface of water made opaque by adding nontoxic white paint. The location of the platform was fixed over a series of trials for each mouse. If

the mouse located the platform within 60 s, the mouse was allowed to remain on it for 30 s. Mice that failed to find the platform within 60 s were manually guided to the platform and allowed to remain on it for 30 s. Mice were given four trials per day for 4 consecutive days (from the second training day to fifth day). A different starting point was used in each of the four trials. The time taken to reach the platform (escape latency) was recorded. A probe test was performed on the sixth day. In the probe test, the platform was removed and each mouse was allowed to swim for 60 s. The number of times the mice crossed the area where the platform had been located was recorded. In all of these experiments, the movement of each mouse was monitored with a CCD camera and processed with NIH IMAGE W.M. software (O'Hara & Co.).

Home-cage activity: The home-cage activity was measured as previously described (66). The mice used in this test were 10- to 12-week-old males. Spontaneous locomotor activity in the home cage (18 cm wide x 14 cm high x 32 cm deep) was determined by utilizing photobeam interruptions by SCANET (6ch SV-20 system, Melquest) for 6 days after habituation to a fresh cage for 24 h. The distance between sensors was 0.5 cm. Mice were housed individually under the 12:12 h LD cycle described above. Food and water were freely available to the mice throughout the experiment. The experiment was begun at 8:00 in the light cycle, and lasted one week.

Open field test and novel object recognition test: The test was performed as previously described (42, 67) with minor modifications. The mice used in this test were 4-week-old males. Locomotor activity was measured with an open field apparatus (60 x 60 cm) at 50 lux (at the surface level of the area). Each mouse was placed in the center of the open field, and its horizontal movements were monitored for 15 min with a CCD camera. The images were processed with NIH IMAGE O.F. software (O'Hara & Co.). The 15-min observation period was divided into three 5-min bins. Total activity in each bin was used in the statistical analysis.

Social interaction test: The social interaction test was performed as previously described

(67) with minor modifications. The mice used in this test were 4-week-old males. Social interaction was measured with the open field apparatus described above. Each mouse used in the test had been placed in the open field for 20 min four days previously. Two genetically identical mice that had been housed separately were placed into the open field apparatus for 20 min. Social interaction was measured by counting the number of particles in each frame with NIH IMAGE O.F. software: the presence of two particles indicated that the mice were not in contact with each other and the presence of only one particle demonstrated contact between the two mice. Total contact times were used in the statistical analysis.

LD transition test: The LD transition test was performed as previously described (68). The apparatus used for the LD transition test consisted of a cage (40 x 20 x 20 cm) equally divided into two by a black partition containing a small opening (O'Hara & Co.). One chamber was open and brightly illuminated, whereas the other chamber was closed and dark. Mice were placed into the lit side and allowed to move freely between the two chambers for 10 min. Time spent in the light side was recorded and analyzed with NIH IMAGE EP software (O' Hara & Co.).

Eight-arm radial maze test: The eight-arm radial maze test was conducted in a manner similar to that described previously (68). The mice used in this test were 5-week-old males. The floor of the maze was made of white Plexiglas, and the wall (10 cm high) consisted of transparent Plexiglas (O' Hara & Co.). Each arm (8 x 40 cm) radiated from an octagonal central starting platform (perimeter 8 x 8 cm) like the spokes of a wheel. Food wells placed at the distal end of each arm remained without food pellets. The maze was elevated 50 cm above the floor and placed at 70 lux. Each mouse was placed in the central starting platform and allowed to explore for a 10 min period. An "arm visit" was defined as traveling for >10 cm from the central platform. For each trial, entries of arms and distance walked were monitored with a CCD camera and processed with NIH IMAGE R.M. software (O'Hara & Co.).

Recording of circadian rhythms: The circadian rhythms were recorded as previously described (69). The mice used in this test were 6-week-old males. Wheel-running was measured with a wheel-meter (WW-3302, O'Hara & Co.), which has 20 sets of a room (14.3 cm wide x 14.8 cm high x 29.3 cm deep) with a wheel-cage (50 cm lap x 5 cm wide). The mouse was able to move freely and was given free access to solid food and water. Every 1/3 revolution of the wheel-cage was recorded as 1 count. The circadian period was calculated by chi-square periodogram.

Neonate survival test: The mice used in this test were 4- to 8-month-old virgin females. In the test to assess neonate survival, pregnant wild-type, *Cadps2*$^{+/-}$ or *Cadps2*$^{-/-}$ females were never touched during pregnancy and were housed separately for at least five days before giving birth. All females were mated with wild-type males. Cross-fostering was performed as previously described (70); briefly, cross-fostering was carried out in the morning when the pups were discovered, and all pups were placed into the recipient female's nest.

Materials. Tetrodotoxin (TTX) (cat. no. 206-11071; Wako) and 2,3-dihydroxy-6-nitro-7-sulfamoyl-benzo(F)quinoxaline (NBQX) (cat. no. 1044; Tocris Cookson) were used. Human recombinant BDNF was a kind gift from Sumitomo Pharmaceuticals. Guinea pig polyclonal antibody against mouse CADPS2 and rabbit polyclonal antibody against mouse CADPS1 were used (10, 11). These anti-CADPS2 (1:10,000 dilution) and anti-CADPS1 (1:5,000 dilution) antibodies were used for Western blotting and immunocyto- and immunohisto-chemistry in this study. Rabbit polyclonal anti-HA antibody (cat. no. 631207; BD Biosciences), anti-synaptophysin antibody (cat. no. RB-1461-P0; NeoMarkers), and anti-CADPS2 antibody (10) were used for immunoprecipitation. The following primary antibodies were also used for Western blotting: mouse monoclonal anti-FLAG (1:2,000 dilution; cat. no. F3165; Sigma), rat monoclonal anti-HA (1:1,000 dilution; clone. no. 3F10; cat. no. 1867423; Roche), mouse monoclonal anti-p150^{Glued} (1:500 dilution; cat. no. 610473; BD

Biosciences), and mouse monoclonal anti-synaptophysin (1:2,000 dilution; cat. no. S5768; Sigma). The following primary antibodies were also used for immunocyto- or immunohisto-chemistry: rabbit anti-BDNF (71) (1:100 dilution), rabbit polyclonal anti-calbindin D-28K (1:1,000 dilution; cat. no. AB1778; Chemicon), mouse monoclonal anti-parvalbumin (1:4,000 dilution; cat. no. P-3088; Sigma), mouse monoclonal anti-chromogranin A (1:1,000 dilution; cat. no. 611844; BD Biosciences), mouse monoclonal anti-synaptophysin (1:200 dilution; cat. no. S5768; Sigma), mouse monoclonal anti-MAP2(2a+2b) (1:1,000 dilution; cat. no. M-1406; Sigma), mouse monoclonal anti-histamine (1:2,000 dilution; cat. no. ab5836; abcam), mouse monoclonal anti-Tau (1:200 dilution; cat. no. 610672; BD Biosciences), and rat monoclonal anti-HA (1:250 dilution; clone. no. 3F10; cat. no. 1867423; Roche).

Supplemental References

63. Wersinger, S.R., Ginns, E.I., O'Carroll, A.M., Lolait, S.J., and Young, W.S., 3rd. 2002. Vasopressin V1b receptor knockout reduces aggressive behavior in male mice. *Mol. Psychiatry.* **7**:975-984.
64. Hironaka, N., Yagi, T., and Niki, H. 2002. Light-potentiation of acoustic startle response (ASR) and monoamine efflux related to fearfulness in Fyn-deficient mice. *Brain Res. Mol. Brain Res.* **98**:102-110.
65. Nishiyama, H., Knopfel, T., Endo, S., and Itohara, S. 2002. Glial protein S100β modulates long-term neuronal synaptic plasticity. *Proc. Natl. Acad. Sci. U. S. A.* **99**:4037-4042.
66. Ohdo, S., Koyanagi, S., Suyama, H., Higuchi, S., and Aramaki, H. 2001. Changing the dosing schedule minimizes the disruptive effects of interferon on clock function. *Nat. Med.* **7**:356-360.
67. Tomemori, Y., Ichiba, M., Kusumoto, A., Mizuno, E., Sato, D., Muroya, S., Nakamura, M., Kawaguchi, H., Yoshida, H., Ueno, S., et al. 2005. A gene-targeted mouse model for chorea-acanthocytosis. *J. Neurochem.* **92**:759-766.
68. Miyakawa, T., Yamada, M., Duttaroy, A., and Wess, J. 2001. Hyperactivity and intact hippocampus-dependent learning in mice lacking the M1 muscarinic acetylcholine receptor. *J. Neurosci.* **21**:5239-5250.
69. Uchihashi, Y., Kuribara, H., Yasuda, H., Umezu, T., and Tadokoro, S. 1994. Long-continuous observation of the effects of methamphetamine on wheel-running and drinking in mice. *Prog. Neuropsychopharmacol. Biol. Psychiatry.* **18**:397-407.
70. Thomas, S.A., and Palmiter, R.D. 1997. Impaired maternal behavior in mice lacking norepinephrine and epinephrine. *Cell.* **91**:583-592.
71. Katoh-Semba, R., Takeuchi, I.K., Semba, R., and Kato, K. 1997. Distribution of brain-derived neurotrophic factor in rats and its changes with development in the brain. *J. Neurochem.* **69**:34-42.
72. Grishanin, R.N., Klenchin, V.A., Loyet, K.M., Kowalchyk, J.A., Ann, K., and Martin, T.F. 2002. Membrane association domains in Ca^{2+}-dependent activator protein for secretion mediate plasma membrane and dense-core vesicle binding required for Ca^{2+}-dependent exocytosis. *J. Biol. Chem.* **277**:22025-22034.

Supplemental Figure Legends

Supplemental Figure 1

Decreased body weight of the *Cadps2*$^{-/-}$ mice. P8 and P21 *Cadps2*$^{-/-}$ (black bars), *Cadps2*$^{+/-}$ (gray bars), and wild-type (white bars) littermates were weighed. The number of animals weighed (*n*) is indicated. The error bars indicate the SEM. **P*<0.05; ***P*<0.01, by Student's *t* test.

Supplemental Figure 2

Decreased spatial memory in *Cadps2*$^{-/-}$ mice. (**A**) Escape latencies of *Cadps2*$^{-/-}$ mice (filled bar; *n*=13) and of wild-type littermates (open bar; *n*=13) in the visible-platform task. Time taken in the last of four consecutive trials was averaged for each genotype. (**B**) Escape latencies of *Cadps2*$^{-/-}$ mice (filled circles; *n*=13) and of wild-type littermates (open circles; *n*=13) in the hidden-platform task during four consecutive days. (**C**) The probe test after the acquisition of the hidden-platform task. Number of crosses over the region where the platform had been located during the probe test is shown. There was no significant difference between wild-type (883.0 ± 95.2 cm, mean ± SEM., *n*=13) and *Cadps2*$^{-/-}$ mice (611.2 ± 91.8 cm , mean ± SEM., *n*=13) in swimming path-length. The error bars indicate the SEM. **P*<0.05, by Student's *t* test.

Supplemental Figure 3

Dark cycle-specific locomotion increase in *Cadps2*$^{-/-}$ mice. Locomotor activity in home cages. After habituation to a fresh cage for 24 h, the locomotor activity of *Cadps2*$^{-/-}$ mice (filled circles; *n*=9) and wild-type littermates (open circles; *n*=9) was measured for 6 days (12 h LD cycle). X-axis shows alternating 12 h LD cycles over six days. The number of photobeam interruptions per 15 min is shown in the Y-axis. The error bars indicate the SEM. **P*<0.05, by Student's *t* test.

Supplemental Figure 4

No difference in anxiety-like behavior of *Cadps2*$^{-/-}$ mice as measured in the LD transition test. (**A** and **B**) Time spent in the light side (**A**) and number of entries to the light side (**B**) of *Cadps2*$^{-/-}$ mice (filled bar; *n*=12) and wild-type littermates (open bar; *n*=14). The error bars indicate the SEM.

Supplemental Figure 5

Decreased locomotor activity and arm entries of *Cadps2*$^{-/-}$ mice in an eight-arm radial maze. (**A**) Locomotor activity in eight-arm radial maze. The locomotor activity of *Cadps2*$^{-/-}$ mice (filled bars; *n*=11), *Cadps2*$^{+/-}$ mice (gray bars; *n*=12), and wild-type littermates (open bars; *n*=13) was measured for 10 min. This test was carried out without food pellets on the arms. (**B**) Number of arm entries of *Cadps2*$^{-/-}$ mice (filled bars), *Cadps2*$^{+/-}$ mice (gray bars), and wild-type littermates (open bars) in (**A**). An "arm entry" was defined as traveling for >10 cm from the central platform. The error bars indicate the SEM. **P*<0.05; ***P*<0.01, by Student's *t* test.

Supplemental Figure 6

Cross-fostering of pups born to wild-type and *Cadps2*$^{-/-}$ females. Pups from *Cadps2*$^{-/-}$ females (*n*=8) were cross-fostered to wild-type females (*n*=8) that gave birth during the same night. Likewise, the pups born to the recipient wild-type females were cross-fostered to the donor *Cadps2*$^{-/-}$ females. Cross-fostering was performed in the morning when the pups were discovered. All pups were placed into the recipient female's nest.

Supplemental Figure 7

Axonal distribution of CADPS2 in hippocampal neurons. (**A**-**C**) Sagittal sections of the

P8 hippocampal CA3 region immunostained for CADPS2 [*green* in (**A**)] and chromogranin A [*red* in (**B**)]. A merged image is shown in (**C**). s.p., stratum pyramidale; s.l., stratum lucidum; s.r., stratum radiatum; CgA, chromogranin A. Scale bar, 10 μm. (**D**-**F**) Sagittal sections of the P8 hippocampal CA3 region immunostained for CADPS2 [*green* in (**D**)] and synaptophysin [*red* in (**E**)]. A merged image is shown in (**F**). Syph, synaptophysin. Scale bar, 10 μm. (**G**-**I**) Hippocampal primary cultures (3 DIV) immunostained for CADPS2 [*green* in (**G**)] and Tau [*red* in (**H**)]. A merged image is shown in (**I**). Scale bar, 30 μm.

Supplemental Figure 8

CADPS2 and BDNF immunoreactivities in mouse hippocampal CA1 region. (**A**-**C**) Sagittal sections of P21 hippocampi immunostained for CADPS2 [*green* in (**A**)] and BDNF [*red* in (**B**)]. A merged image is shown in (**C**). s.o., stratum oriens; s.p., stratum pyramidale. Scale bar, 20 μm.

Supplemental Figure 9

CADPS2 and CADPS1 expression in human leukocytes. (**A**-**D**) Leukocytes from the blood of healthy human subjects were fractionated and immunostained for CADPS2 [*green* in (**A**)], histamine [*red* in (**B**)], and CADPS1 [*blue* in (**C**)]. Merged fluorescence data (*green*, *red*, and *blue*) over a DIC image are shown in (**D**). The white arrow points to a histamine-positive basophilic leukocyte expressing both CADPS2 and CADPS1. Scale bars, 500 μm.

Supplemental Figure 10

Schematic representation of suggested BDNF release manner from wild-type neuron, *Cadps2*$^{-/-}$ neuron, and CADPS2(Δexon3)-expressed neuron. (**A**) CADPS2 plays a role in BDNF release in wild-type neuron at the soma and axon terminal. (**B**) BDNF release is

substantially decreased in *Cadps2*$^{-/-}$ neuron. (**C**) CADPS2(Δexon3) is localized at cell soma and not transported to presynaptic terminal, suggesting augmented BDNF release from cell soma and decreased BDNF release from the axon terminal.

Supplemental Figure 11

Schematic representation of human CADPS2 protein and nonsynonymous mutations. Seven novel nonsynonymous (missense) mutations in this report are shown. Represented here are the C2 and PH-like domains, Munc13-1 homologous domain (MHD), and C-terminal domain that mediates dense-core vesicle binding (C-tail) (72). Amino acid positions are based on human CADPS2 (NCBI accession number NP_060424).

Supplemental Table 1

Sensory functions of *Cadps2*$^{-/-}$ mice

Phenotype	**Status**
Visual test	
wild-type (*n*=8)	Normal
Cadps2$^{-/-}$ (*n*=8)	Normal
Olfactory test (time to find cookies)	
wild-type (*n*=8)	234.5±56.5 s*
Cadps2$^{-/-}$ (*n*=8)	209.1±39.5 s*
Auditory test (% change of movements to the sound stimulus)	
wild-type (*n*=16)	78.7±14.7%*
Cadps2$^{-/-}$ (*n*=12)	76.2±10.2%*

Values are mean ± SEM.

*There was no significant difference between wild-type and *Cadps2*$^{-/-}$ mice.

Supplemental Table 2

CADPS2 nonsynonymous mutations identified in autistic patients

individual code[a]	**sex**	**nucleotide change**[b]	**amino acid change**[c]
AU004804	male	T2405C	I761T
AU0943302	male	G2419C	V766L
AU1182302	male	C2504A	T794N
AU0803301	female	A2896G	T925A
AU013304	male	G3286A	D1055N
AU069603	male	G3286A	D1055N
AU009203	male	G3457A	D1112N
AU048204	male	C3722T	T1200M

All autistic patients examined were white.

These mutations were not observed in 218 biologically unrelated white subjects from cohorts recruited as bipolar disorder pedigrees.

Note that the currently detected nonsynonymous mutations were all heterozygous.

[a]These numbers are those of the Autism Genetic Resource Exchange (AGRE).

[b]Nucleotide positions are based on the human *CADPS2* gene (NCBI accession number NM_017954).

[c]Amino acid positions are based on human CADPS2 protein (NCBI accession number NP_060424).

Supplemental Figure 1

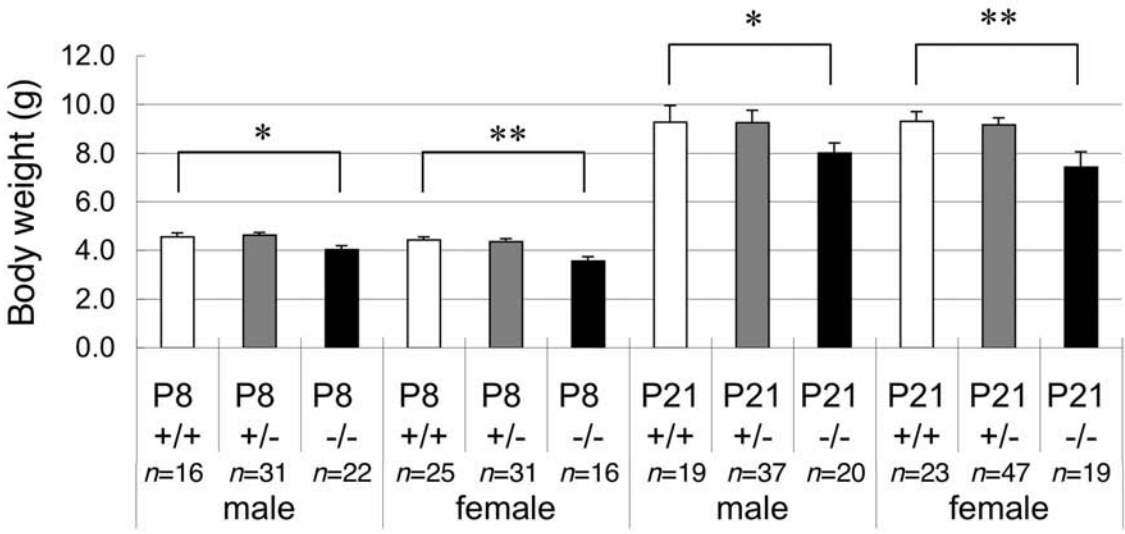

Supplemental Figure 2

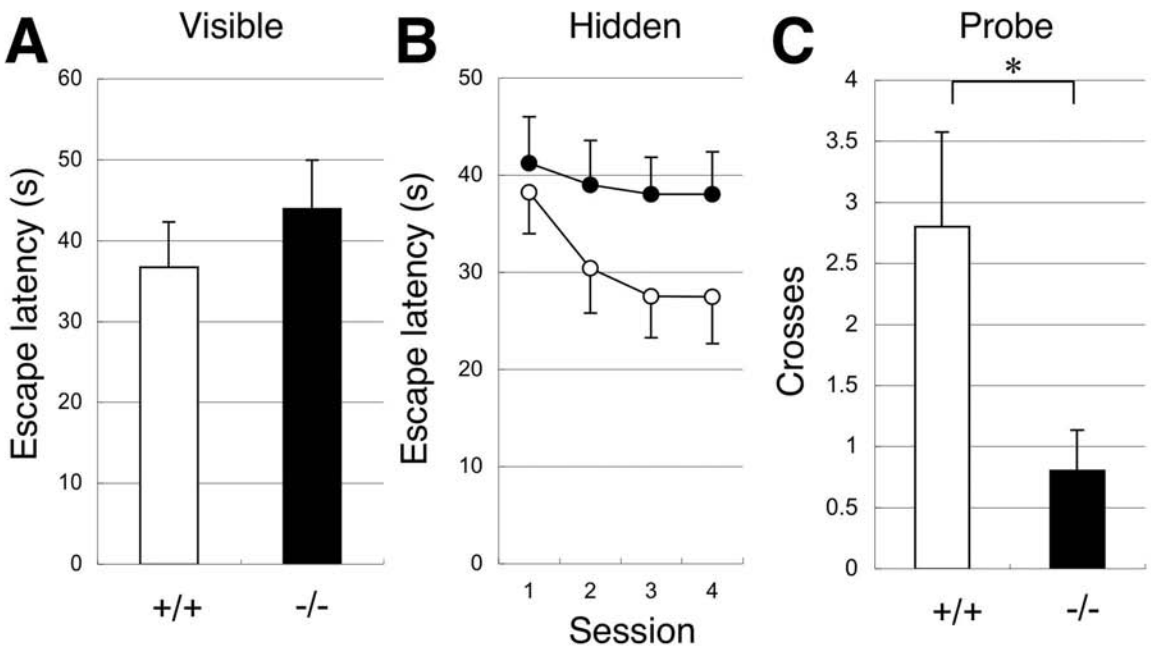

Supplemental Figure 3

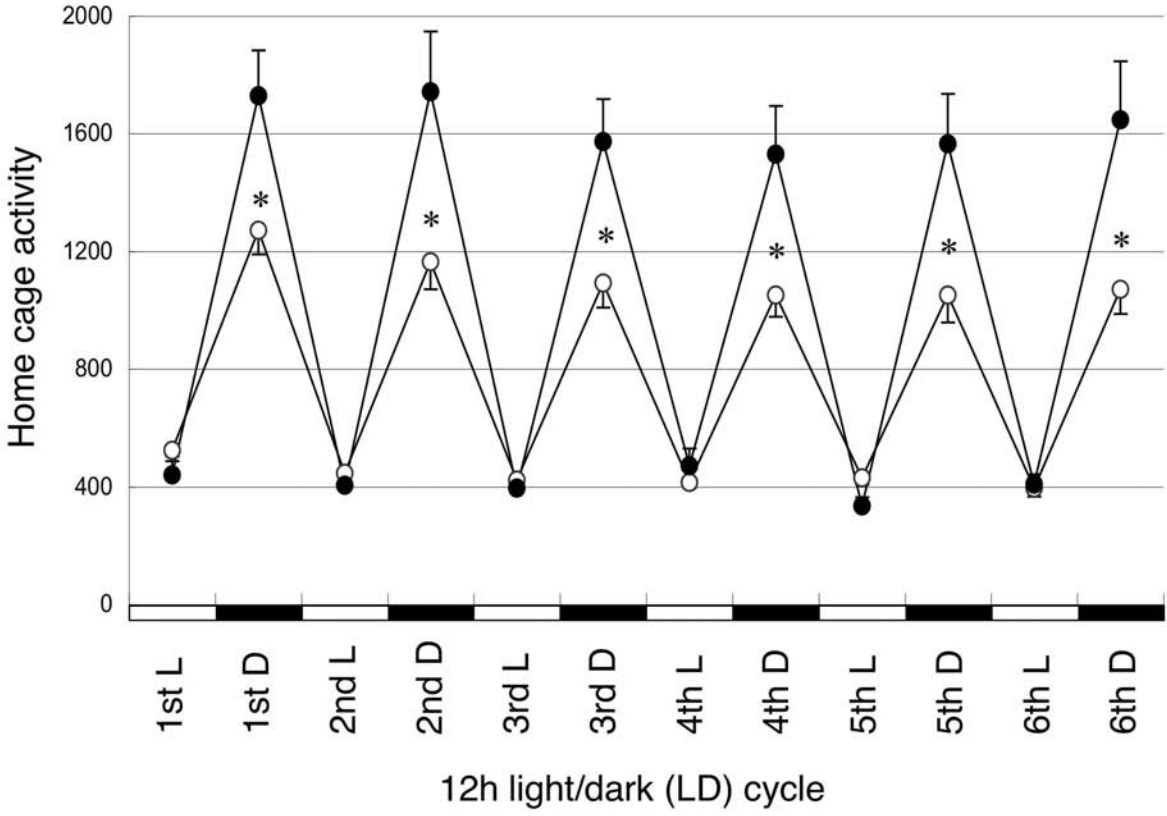

Supplemental Figure 4

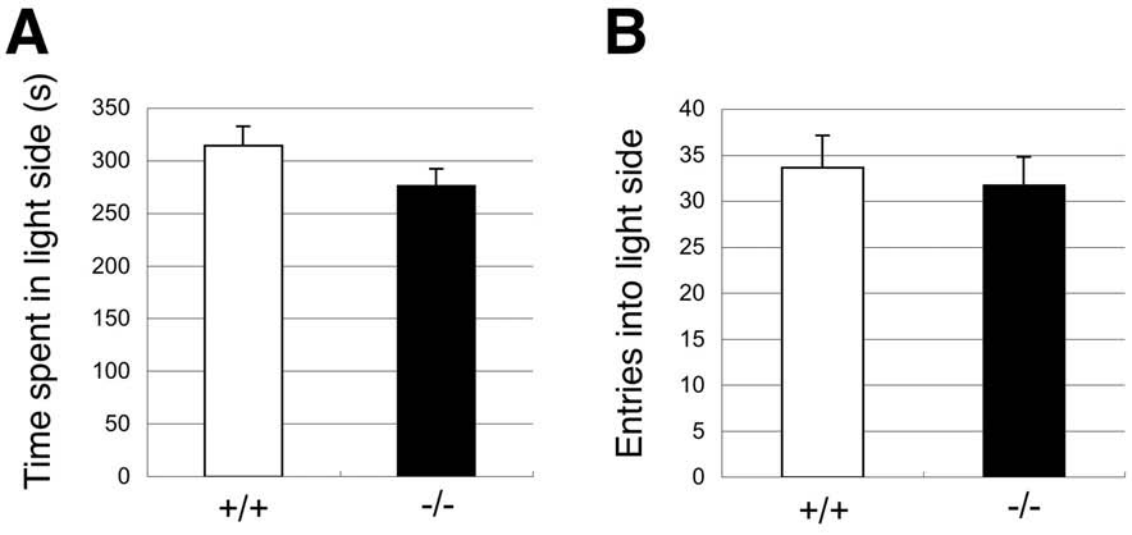

Supplemental Figure 5

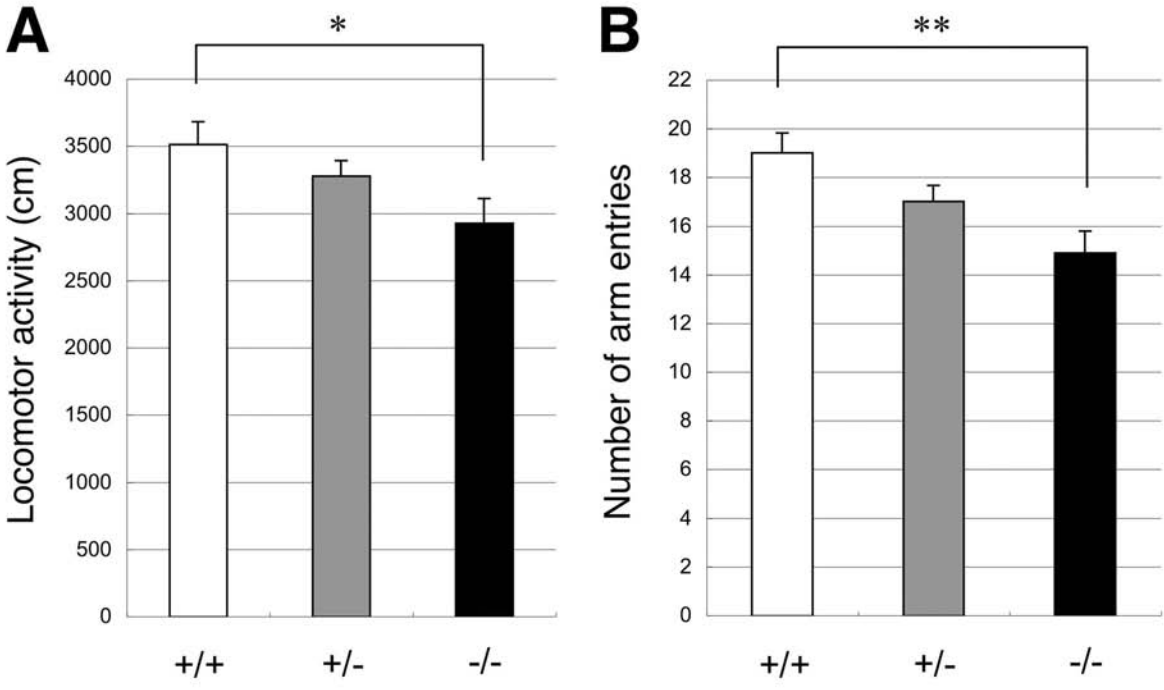

Supplemental Figure 6

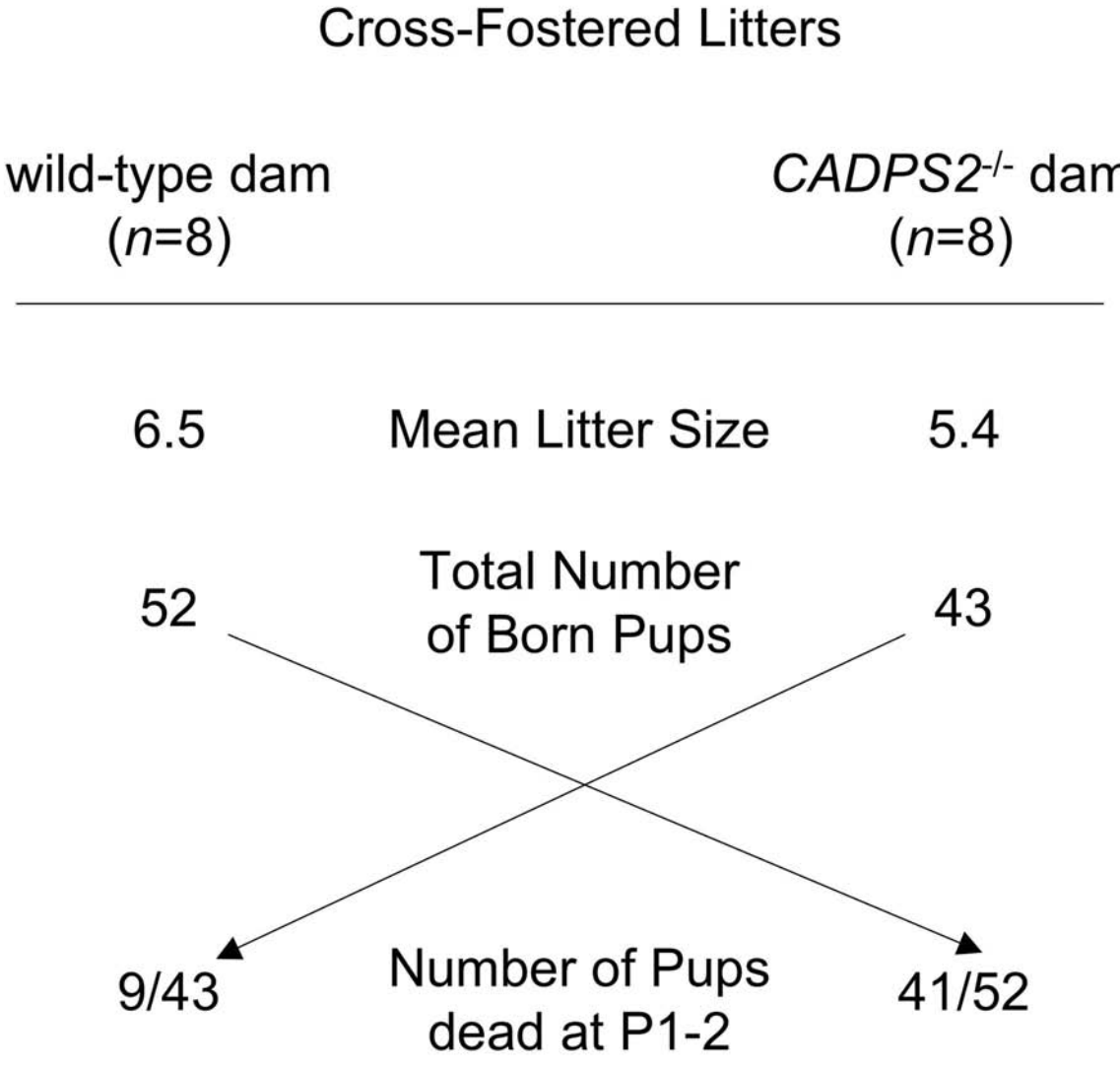

Supplemental Figure 7

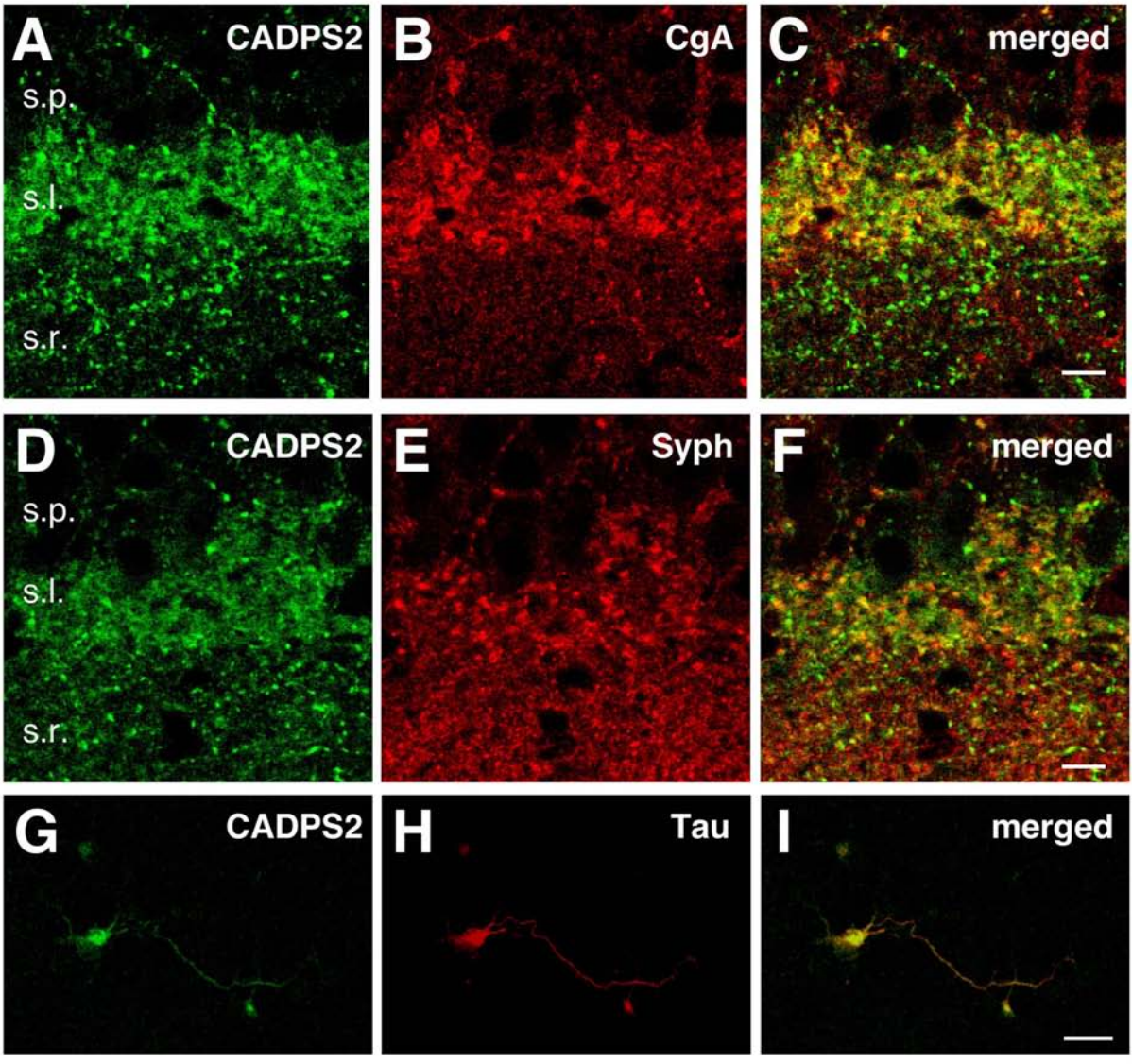

Supplemental Figure 8

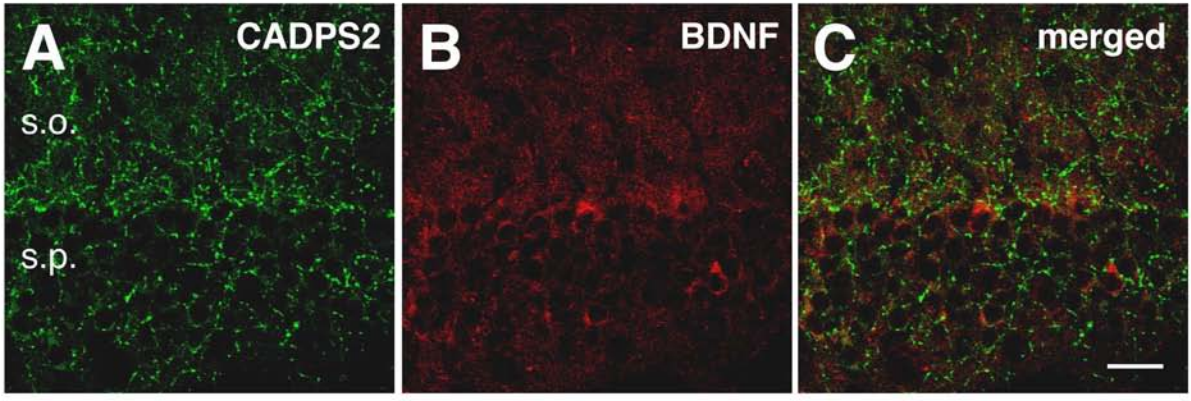

Supplemental Figure 9

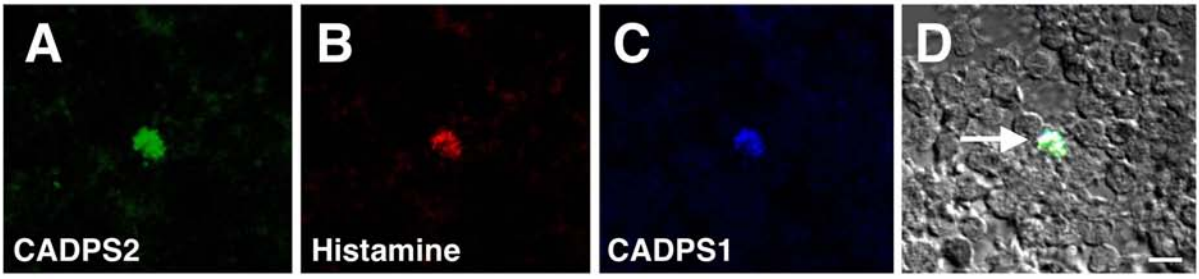

Supplemental Figure 10

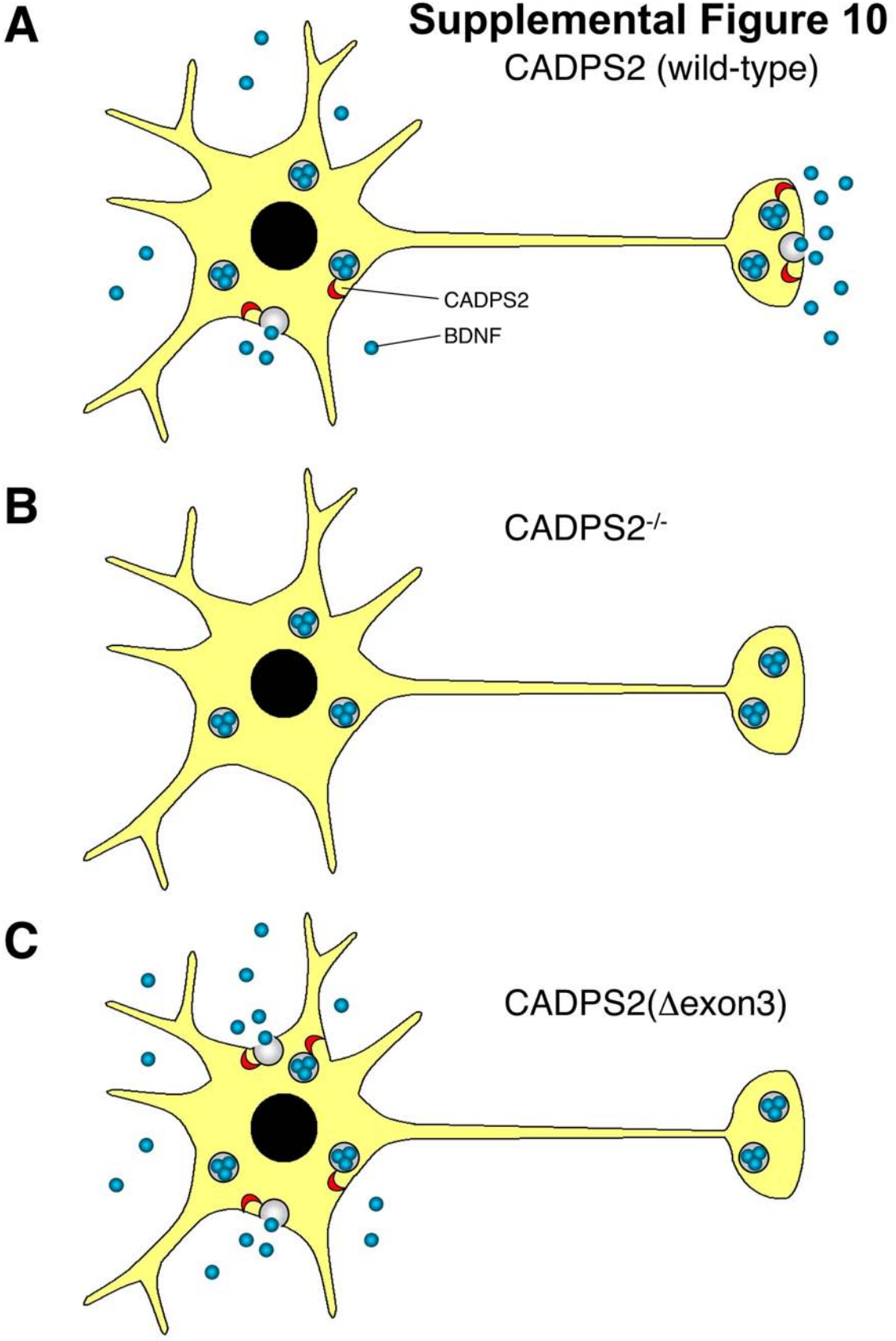

Supplemental Figure 11